A Contour Deformation Model of Capacitance VideoDisc Signal Pickup

P. D. Southgate
RCA Laboratories, Princeton, NJ 08540

Abstract—A method of calculating the videodisc pickup signal is described that includes the elastic deformation of the disc by the stylus. The stylus shoe is idealized to a flat, rectangular shape and small vertical displacements are assumed. Disc-stylus capacitance is calculated using a two-dimensional geometry and an approximation to the field configuration that allows fast computation. Typical results are described for the wavelength and tracking-force dependence of pickup. There is agreement between most general features of calculated and measured pickup. The mechanism of soundbeat is investigated and shown, within the terms of this model, to depend primarily on the elastic deformation of the signal contour. The calculated magnitude and the wavelength dependence of soundbeat agrees well with measurement; for a "flat-top" signal, drop of soundbeat and change of wavelength dependence of the type observed are predicted. Calculations usually deviate from measurements only by a magnitude similar to the mutual deviation of measurements made under varying conditions.

Introduction

The successfully optimized combination of stylus configuration and signal depth used in the capacitance pickup VideoDisc system has been developed by exhaustive experimental trial in conjunction with idealized models of electrode-disc capacitance. These models, although providing substantial insight into the pickup mechanism, are not complete, since they do not fully take into account the elastic deformation of the disc surface by the stylus. Since, as will be seen, deformation has a major effect in modifying the signal contour, particularly with regard to second-order effects, such as harmonic gen-

eration and soundbeat, it is of considerable interest to include this deformation. In this paper, a model is developed that represents the deformation, with some approximations that are geometrical in nature and are believed to be small. The model is simplified by representing the disc surface as a perfect conductor with a thin dielectric layer on top; gradations and fluctuation noise in the conductive layer are not included. It is also assumed that the stylus tip is surrounded by the lubricating oil so that signal-frequency fluctuations in the oil surface contour do not affect the electrode-disc capacitance.

Some general features of the signal pickup predicted by the model will be described and compared with measurements made by a number of workers in RCA Laboratories. The correspondence with measurement is usually reasonably good, within the variability of the measurements. Small systematic differences may be caused by the geometric approximations made in this analysis; a greater difference probably arises from an inadequate accounting of the oil film behavior, both in its viscoelastic properties and its varying dielectric effect. A full treatment of this would be very difficult; the model is therefore presented as a demonstration of how closely stylus performance can be predicted with only an elementary inclusion of these effects.

Other models, using different approximations, have been described in the past. The basis of these has been indicated by Clemens;[1] the analysis has been extended considerably in unpublished work by J. J. Gibson, J. R. Matey, and R. W. Nosker.

Elastic Contour Deformation

Computation of the deformation due to the stylus is reduced to manageable proportions by using an idealized stylus form. Fig. 1 compares this form with the real stylus. The grooves are flattened and the contact area of the shoe has a straight rather than an acute leading edge. The shoe shape transverse to the groove direction is taken to be slightly rounded so that the pressure under the shoe does not depend on the distance from the groove center. Calculations of vertical surface-contour deformation are made at points along the groove center; it can be shown that if the location is moved toward the side of the shoe, the deformation will not change much until it is close to the side.

The elastic modulus used is the low-strain time-independent value; yield, relaxation effects, and inertial effects are ignored. Although the total stress near the stylus contact at the tips of the

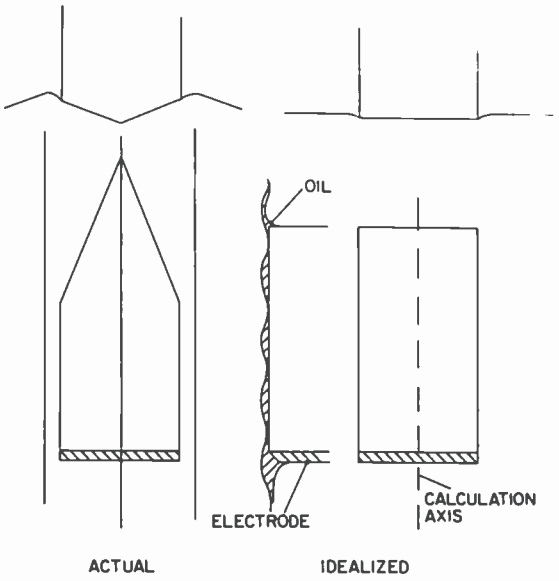

Fig. 1—Idealized form of stylus, used in calculations, compared with real stylus. Electrode and signal depth is approximately to scale; distribution of oil is assumed.

signal elements can be large, the smaller shear component, which would lead to yield, usually does not exceed the yield stress. In addition, it is transient, and the short-term yield stress in disc material has been shown to be much higher than the static value. The material damping has been shown to be low at frequencies of the order of 1 MHz, justifying the neglect of relaxation effects. Inertial effects are not important, because the speed of sound is about 400 times the speed of the disc, so that the elastic deformation is always near equilibrium.

In addition to its possible dielectric effects, the lubricating oil can modify the pressure distribution under the shoe if it is sufficiently viscous. The bulk viscosity is of the order of 0.2 poise at low shear rates and probably considerably less at the high rates obtaining between the shoe and disc. Simple calculations show that for normal video signals, where the channel space between the shoe and the disc is 800 Å or more, the normal stylus pressure will cause the oil to flow laterally outward in a time short compared with the transit time of the disc under the shoe. The pressure profile near the electrode will therefore be little modified by the oil. For signals of shallow modulation depth, however, oil flow may be slower; for a smooth groove and oil of viscosity 0.1 poise, an initial thickness of

400 Å will be reduced to 250 Å only after the oil has traversed the whole way under a 4μm long shoe. It is likely therefore that the oil under these conditions will cause the pressure under the leading part of a shoe, which is essentially parallel to the disc, to be a little greater than that under the following part. The oil may also contribute an essentially elastic thin surface layer; this layer will be included in the surface dielectric of the disc material. Errors introduced by the above approximations are believed to be small but are difficult to assess; it would require a comparison with exact calculation for some configurations, a formidable task which has not been attempted.

A point force F perpendicular to a horizontal semi-infinite elastic solid surface produces a vertical deflection at distance r, if F is small, of

$$z = F(1 - \nu^2)/\pi E r, \qquad [1]$$

where E is Young's modulus and ν Poisson's ratio. If the stylus shoe is divided into strip elements as shown in Fig. 2, then the vertical deflection at a point on the groove center due to one of these elements may be obtained by integrating the deflection of Eq. [1] over the element, which is assumed to apply a constant vertical pressure to the disc surface. It is convenient to use two analytic approxi-

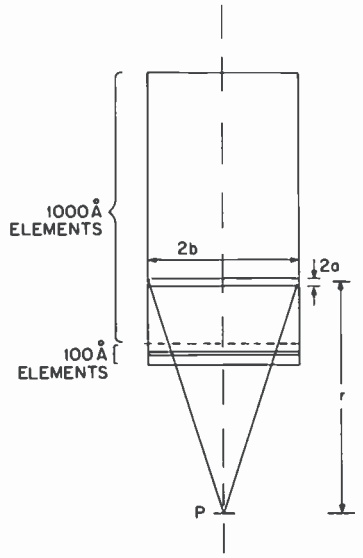

Fig. 2—Shoe-area element dimensions.

mations to this integral. One is for a close element of width $2a$ comparable to its distance r from the point considered.

$$z = \frac{F}{b\pi}\frac{(1-\nu^2)}{E}\left(\frac{1}{2a}[(r+a)\ln(r+a) - (r-a)\ln(r-a)] - 1 - \ln 2b\right); \quad [2]$$

the other approximation is for more distant elements,

$$z = \frac{F}{b\pi}\frac{(1-\nu^2)}{E}\frac{1}{2}\ln\frac{(1+r^2/b^2)-1}{(1+r^2/b^2)+1}. \quad [3]$$

Here F is the total force on the element and a and b are its half width and length. The b/a ratios used in these calculations (20 or greater) give a sufficiently large region of overlap between these two approximations.

If the number of elemental spaces between the force and the deflection point is $k = r/2a$, then the interaction coefficient is defined as $I(k) = z/F$, given by the appropriate Eq. [2] or [3]. The total displacement at the location of element j along the axis due to a set of forces $F(i)$ at location i will then be

$$z(j) = \sum_i F(i)\, I(i-j). \quad [4]$$

Incorporation of a disc surface signal modulation into these calculations proceeds as in Fig. 3. The upper diagram shows the signal surface contour before stylus pressure is applied, the mean plane of the disc being indicated by the broken line. When the pressure is applied, the disc mean plane is depressed by the sum of the stylus depth below the initial mean plane and the signal contour modulation, if the stylus is in contact with the disc. The situation is shown in the lower diagram. In these calculations, the elastic strain in those parts of the disc between the surface and the mean plane is ignored. Region A (Fig. 3) is assumed to be stiff in the vertical direction (so that $d_1 = d_2$) but not to contribute otherwise to the disc stiffness; region B is taken to contribute to disc stiffness although it is in fact not present. Fig. 3 suggests a greater error from this cause than is the case, since the vertical scale is exaggerated; the error can be shown to be small and comparable to that produced by the implicit assumption of Eq. [1] that the vertical displacements are small compared with the horizontal scale.

The procedure followed to calculate surface contour deformation, then, is first to consider only those elements in contact with the shoe. The vertical displacements of the disc surface at the locations

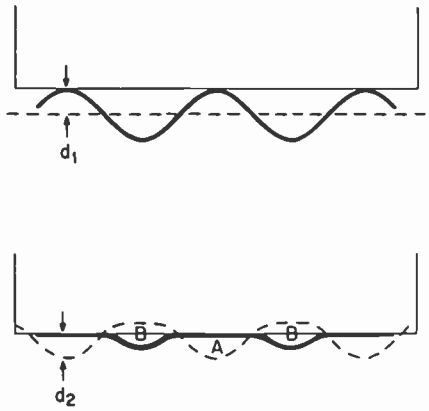

Fig. 3—Elastic deformation of mid-plane of disc surface showing regions of material in which the compression is ignored.

will be the sum of the stylus depth below the mean disc plane and of the modulation. Thus, in the set of Eqs. [4], if the range of i and j is restricted to only the contact points, all values of $z(j)$ are known, so that this forms a complete and solvable set of equations. The set may then be inverted to give the $F(i)$ values.

This procedure is followed iteratively. At first, a convenient set of points under the stylus but near the signal peaks is chosen. Eqs. [4] are solved and the derived $F(i)$ values are used to obtain the surface contour at all points under the stylus. Two physically unrealistic situations may then be found: the disc surface may be above the shoe or the force may be negative (so that the surface is pulled up toward the shoe). Points of the first kind are added to the original set and points of the second kind are removed, forming a new set of final contact points. Further iterations are then made until all forces are positive and all disc surface locations are at or below the shoe surface. Given this final set of forces, the desired calculation of the deflection of all points on the disc surface can be made.

It is only close to the electrode that a small element size is needed to give accuracy in the final capacitance calculations. In the calculations to be described, the elements within 2000 Å of the electrode-stylus interface are 100 Å wide, and elsewhere they are 1000 Å, as indicated in Fig. 2. Interaction coefficients are scaled to accommodate this change of size.

To produce a varying stylus tracking force, the depth of the shoe below the average disc surface is varied. It is a feature of these computations that the tracking force cannot be specified in advance;

reasonable estimates must be made and the final results for the desired tracking force found by interpolation. The curvature of the stylus shoe can vary depending on its playing-wear history. An assessment of the stylus shoe profile can be made from scanning electron microscope (SEM) observations. When this is known for the particular shoe used, or for one that has had a similar history, an analytic form can be fitted to the observed profile and this form can be used in the deformation calculations. Alternatively, a "standard" shoe profile is sometimes used, which is the profile that gives a uniform pressure on a signal-free disc at 65 dyne tracking force. This profile may be increased by a "curvature factor" S.

General Features of the Calculated Deformation

The type of signal for which pickup is most affected by the details of elastic deformation is the low-amplitude audio-only signal played by a shoe of low curvature. The shoe is here in contact with the disc surface along almost its whole length, so that there is no modulation at the electrode-stylus contact plane. It might be expected that this would lead to a very low value of capacitive pickup from the electrode. Further examination shows, however, that the variation of pressure as the signal passes under the shoe produces an enhanced "bulge" close to the pressure edge. The situation is shown in Fig. 4, where the surface configuration is given for 12 successive phases of the signal. The vertical scale is exaggerated by 14 times. The broken line, for reference, gives the dimple that would be produced in a smooth disc. In addition, the pressure profile is plotted. It can be seen that the pressure fluctuates greatly at the edge; in fact, there is a mathematical singularity there, and at the limit of infinitesimal element size the pressure will swing between zero and infinity. It is this sharp change of pressure that causes the local bulge, so that 2000 Å from the edge, the surface modulation is quite large, even though this distance is small compared with the signal wavelength. Since the electrode extends out 2000 Å, the enhanced modulation produces capacitance pickup.

This model therefore provides an answer to the question of why significant audio-only pickup can be obtained even though the signal elements are completely compressed by the stylus. For a standard video signal, the modulation depth is larger, so that complete compression does not occur; in this case the effects of finite elastic distortion are less obvious. In addition, a real stylus-shoe is more rounded near the electrode than is the constant-pressure profile used for Fig. 4. Fig. 5 shows one phase of two similar video + audio

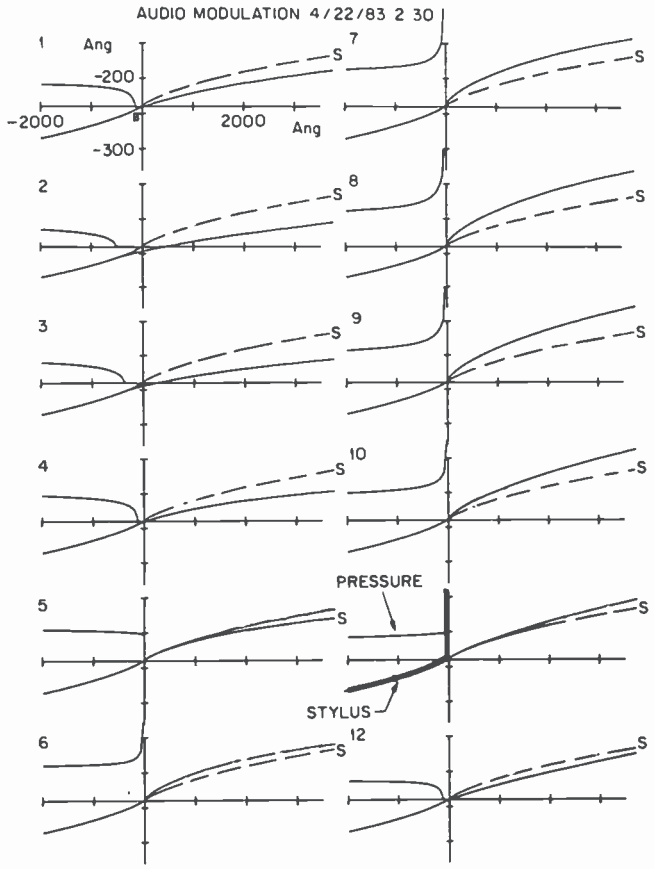

Fig. 4—Surface contour for twelve equally spaced phases of a audio-only signal near the pressure edge. The pressure profile and the stylus outline are identified in phase 11 (vertical/horizontal scale ratio = 14).

signals, with a modulation depth of 850 Å and a wavelength of 1μm. The "flat-top" signal will be described later. For the phase shown, the disc surface contacts the shoe near the electrode, and the deformation in that region will depend quite strongly on various parameters such as the tracking force. For much of the remainder of the cycle, the electrode-disc spacing will be less sensitive to these parameters. The calculated pickup amplitude will therefore usually not vary greatly from that obtained by more simplified assumptions on the conformation of the surface. What will differ are the second-order effects—harmonic distortion, signal intermodulation, sound-

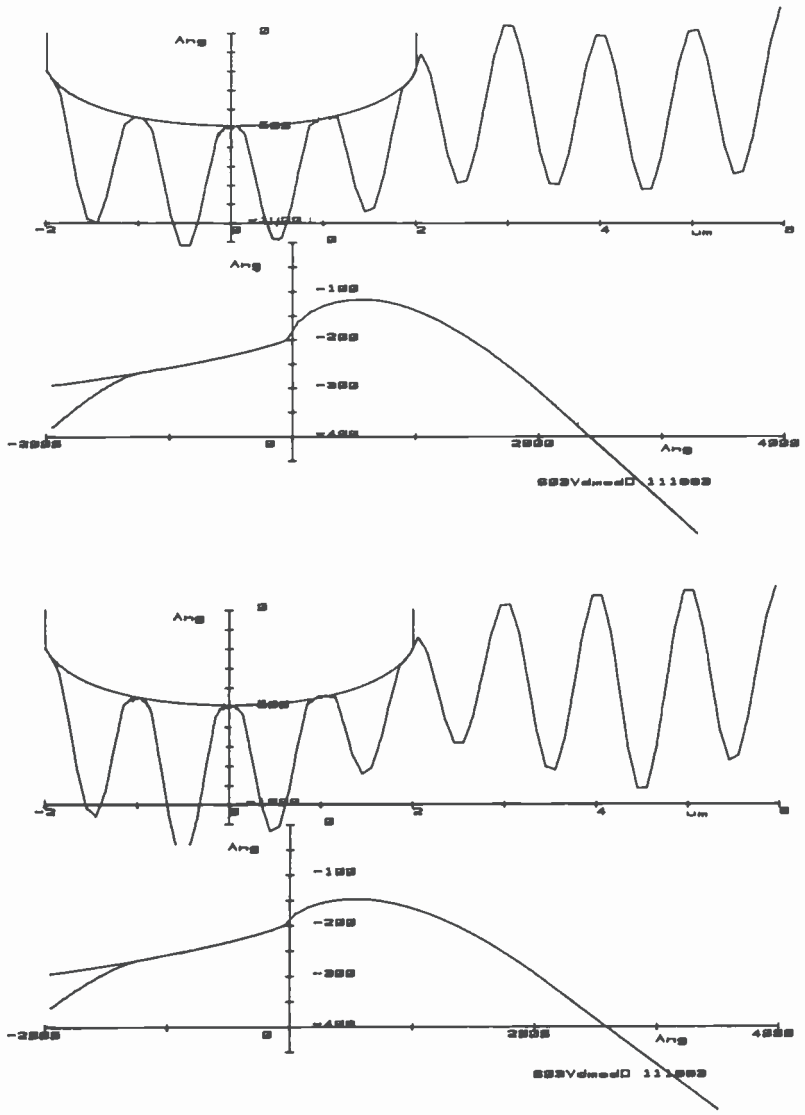

Fig. 5—Surface contours, over the whole shoe and on a magnified scale near the pressure edge for video plus audio signal. Top shows normal signal and bottom "flat top" signal.

beat and the dependence of these on wavelength, tracking force, shoe length, and shoe curvature.

Capacitance Pickup

Having obtained the surface contour, the capacitance between the stylus electrode and the disc (assuming a two-dimensional situation) may be computed exactly using a field distribution program based on Poissons equation. Calculations of this kind have been carried out by N. Binenbaum and R. W. Nosker of these laboratories for the case of a trapezoidal signal form. Significant contributions to the capacitance modulation occur only within about 1 μm of the electrode, so calculations can be confined to this region. In the present paper the electrode is represented as having an angled end and a step-back from the stylus shoe edge, which is a reasonable representation of the form often seen in SEM displays. In addition, the conducting surface of the disc is taken to be displaced below the contact surface due to an intervening dielectric layer (the surface vinyl above the contacting graphite grains) and possibly to an adherent monolayer of oil. Fig. 6(a) shows the dimensions involved.

The exact capacitance calculation involves significant computer time. Again, for the numerous configurations, with the different signals, phases, and electrode shapes needed in this investigation, simplified calculation is desirable. An approximation is used here in which a reasonable estimate is made of the shape of the field lines and of the variation in length of these lines computed as the signal contour passes under the electrode. The contribution to the total capacitance from the element containing the line will then vary inversely as the length of the line, suitably weighted by the dielectric constant.

The dielectric gap is divided into elements bounded by the field lines as shown in Fig. 6(b). The capacitance of each element can then be calculated approximately from its average cross-section area and the length of the lines. Errors in this method will be least in the region where the parallel-plate situation is approximated as in region III of Fig. 6(b), which in fact contributes the majority of the capacitance variation. The shape of the field lines in region III is taken as straight and parallel to the vertical electrode face. In regions I and II, the lines are taken as arcs of a circle for the more distant elements. For elements that are closer than three times the shoe-disc gap on the after side of the electrode, the elements grade from circular arcs to straight lines. An interpolation for both ele-

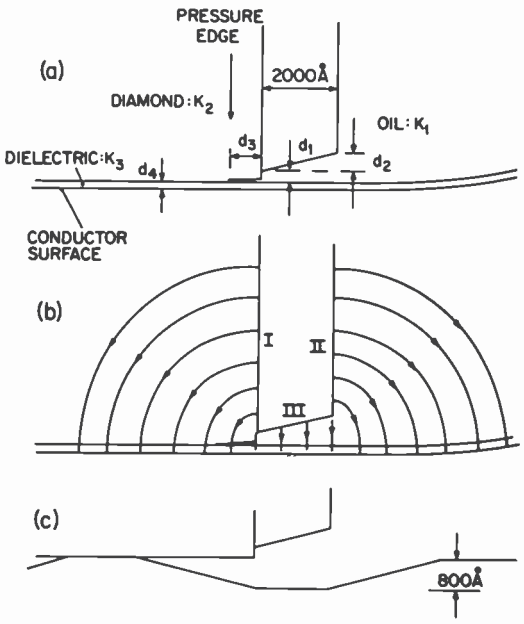

Fig. 6—(a) Identification of electrode and disc spacing dimensions; (b) approximation used for field configuration; and (c) trapezoidal waveform used to check approximate calculations.

ment length and width is made between these two forms for the intermediate elements.

An approximation of this kind can be expected to be only moderately accurate for calculations of absolute capacitance. However, for perturbations of this capacitance, such as are given by the signal form on the disc, a higher accuracy can be expected. An independent derivation of the expected error would be difficult to make, but comparisons with exact calculations for specific forms give a good idea of the general accuracy. Table 1 shows the results of Binenbaum and Nosker for the trapezoidal waveform shown in Fig. 6(c). Using 11 phases of this wave, limited to a 1½ wavelength segment, they derived values of capacitance modulation and its second and third harmonic content for a number of electrode shapes. Table 1 also shows the result of the approximate calculations just described. Fourier analysis of the capacitance values gives fundamental and harmonic pick-up components, which in this paper will be quoted in dB relative to $1aF$ ($10^{-18}F$) RMS (designated dBR) and dB relative to the fundamental, respectively. The approximate results

Table 1—Comparison of Approximate (B) with Exact (A) Electrode-Disc Capacitance Calculations

Electrode and Dielectric Dimensions (Å)				Fundamental (dBR)		Harmonics dB Relative to Fundamental 2nd		3rd	
d_1	d_2	d_4	k_1	A	B	A	B	A	B
200	200	200	2.4	32.9	33.5	−16.6	−16.7	−37.5	−32.0
0	0	200	1	42.1	42.3	−8.8	−8.8	−21.9	−23.3
200	2000	200	2.4	28.2	29.2	−14.7	−14.6		−26.7
200	200	700	2.4	22.7	23.6	−22.7	−21.6		−42.9

agree quite well with the exact values, particularly in the second harmonic content of the pickup. Greater error is seen in the third harmonic at low levels; it is of the order of 1% of the fundamental and is comparable with errors expected from the finite number of sampling points. Agreement is good even when the electrode-disc spacing is as large as 700 Å, in which case the field configuration used in the approximation will differ significantly from the true configuration. The approximate calculations will be used in the remainder of the work to be described.

Calculations of deformed contour and, from them, of capacitance, are made for single sine waves of various amplitudes and wavelengths at each of 12 phases of the wave.

More complex signals, composed of video and audio superposed, are arranged to have an integral number of video wavelengths in an audio signal to minimize calculation of one complete cycle of the total signals. Again, 12 phases of each video cycle are taken. These signals are analyzed by bandpass filtering and computation of the zero-crossing points of the filtered video waveform. Subsequent Fourier analysis then gives the fundamental (i.e., audio-frequency) component of these zero-crossing deviations. Soundbeat, which is the phase modulation of the video carrier pickup by the superposed audio carrier, may then be calculated from the zero-crossings. For a waveform phase-modulated by

$$\cos(\omega_v t + \Delta\phi \cos \omega_a t),$$

soundbeat (in dB) is defined as

$$20\log(5\,\omega_a\,\Delta\phi/\omega_v).$$

The filtering action removes some components that contribute to soundbeat; these are restored by adding a small correction to the value directly calculated from the zero crossings.

Pickup of Single-Frequency Signals

In general, for a constant modulation depth, calculated pick-up tends to increase steadily with the modulation depth and to fall off at long and short wavelengths. The dependence on tracking force is more complex; it may increase, decrease, or go through a maximum. The results to be described have been calculated using a disc Young's modulus of 5.4×10^{10} dyne cm^{-2} and a Poisson ratio of 0.35, near the values measured at 15 MHz by Rehwald and Vonlanthen of RCA Laboratories, Zurich. Fig. 7(a) and 7(b) show the calculated pickup from a sinusoidal signal as a function of tracking force, with separate plots for two different shoelengths (1 dyne is approximately 1 mg force). The electrode is of form E2 [Table 2 and Fig. 6(a)] and the stylus curvature factor is 2. Decrease of pickup with increased tracking force is strongest for long wavelength and

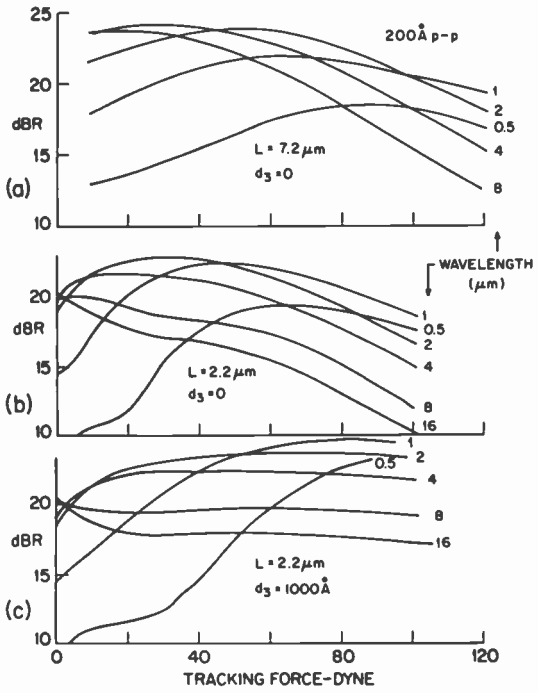

Fig. 7—Effect of tracking force variation on calculated pickup, of a 200 Å p-p signal with wavelengths of from 0.5 to 16 μm. Two shoe lengths L and pressure edge set-back d_3 are shown.

Table 2—Electrode and Disc Dielectric Dimensions (See Fig. 6)

Electrode designation	d_1	d_2	d_3	d_4
E1	200	500	0	200
E2	300	1000	0	200

small signal depth, that is, when all angles to the horizontal are minimized. The increased tracking force then compresses the signal contour. The opposite effect of increased signal with increasing tracking force is seen for short wavelength and large signal depth, where the dominant effect is to bring the electrode closer to the disc surface rather than to compress the contour. Changes of electrode form, or thickness of disc surface dielectric layer, will change the magnitude of the pickup amplitude but, within limits, do not have a large effect on the shape of the curves. A set-back of the pressure edge or an increase of shoe length both tend to decrease the effect of tracking force variation. Fig. 7(c) shows the marked flattening that occurs with a pressure-edge set-back of 1000 Å. A set-back of this magnitude would be difficult to detect experimentally; the difference between Fig. 7(b) and 7(c) therefore illustrates the caution that should be exercised in comparing calculation with experiment.

Curves similar to those of Fig. 7 can now be used to obtain the pickup at constant tracking force. A typical variation with wavelength is shown in Fig. 8 for a signal depth of 200 Å p-p. Calculated curves are shown as dashed lines and are compared with measured curves (solid lines). The electrode gap value has been adjusted to give approximately the same pickup magnitude as measured; these values are in the 300 to 800 Å range and correspond roughly to those estimated from SEM observations in each case. A "standard" shoe shape with a curvature factor of 2 has been used. The tracking force is 60 dyne for the top two curves and 40 dyne for the lower curve. These adjustments from the total applied tracking force of 65 dyne have been made to account for a proportion of the force supported by oil and debris outside the shoe area, guessed to be 10%. For curve C in Fig. 7, the shoe width is 40% greater than that for curves A and B. In addition the shoes have been given a slight tilt to stimulate a possible wedge action of the oil film, as discussed before; the prow end is 150 Å lower than the electrode end of the shoe.

The curves show a fall-off at both short and long wavelengths. At the longer wavelengths the signal profile can conform more closely

to the shoe and so a fall-off can be expected, beginning at wavelengths comparable to the shoe length. At short wavelengths, the effective electrical aperture of the electrode capacitance becomes comparable with the wavelength and this reduces pickup. However, for the shorter shoes, the calculated fall-off is less than measured. One factor that could change the fall-off rate is the assigned electrode gap. This does not seem to be responsible, however, since a change of gap that produces a large deviation of absolute value of pickup from that measured does not produce a significantly better shape match. A second possible factor is the skewing of the electrode edge line from the signal peak ridge. This also cannot explain the difference, since a skew sufficient to produce a 3dB change in output would also produce a sharp change in the slope of the pickup versus wavelength curve, which is not seen in the measurements. Different shoe shapes and tracking force, within limits that reasonably correspond to measurement, do not produce a significantly better fit to measurement than seen in Fig. 8.

Measurements of dependence of pickup on signal amplitude, using a shoe of 5.2 μm overall length, are shown in Fig. 9. Comparable calculations for wavelengths of 1 and 8 μm are shown as dashed lines, using a shoe of profile matched to SEM measurements and with a corresponding effective length of 4.6 μm. The stylus is given an 80 Å tilt and 60 dyne tracking force. The most noticeable characteristic of the measurements is the flattening of the curve at higher amplitudes, which occurs more strongly at the shorter wavelengths. A similar effect is seen in the calculated curves at 1 μm wavelength. The linearity of the 8 μm calculated curves, however, is at variance with the slight curvature measured at both 4.2 and 13.3 μm, at which wavelengths the original signal is believed to be well-calibrated. Various stylus and electrode shapes have been tried, but all give curves close to linear; this discrepancy also has not been resolved within the framework of the model.

Comparison of the measured harmonic content of pickup with calculations using the same shoe profile as in Fig. 9 is given in Fig. 10. The electrode gap again was adjusted to give the same magnitude of the pickup amplitude as measured. The calculated magnitude of both second and third harmonic is of the same order as measurement at higher signal amplitude; at low amplitudes, the calculated harmonics do not fall off as rapidly as measured. Below −30 dB, calculation is not expected to give accurate results. In some regions, a rapid change of harmonic content with tracking force was calculated, in which case harmonic levels were averaged over the 50- to 70-dyne range.

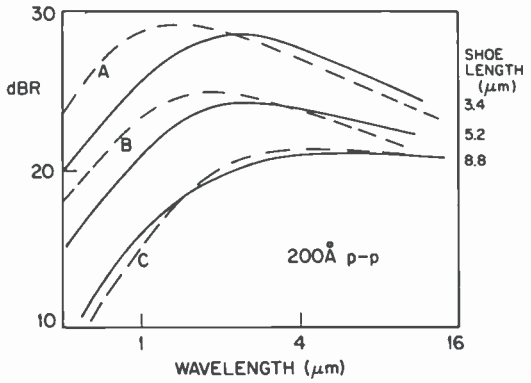

Fig. 8—Calculated variation (dashed lines) of pickup of a 200 Å p-p signal with wavelength compared with measurement (solid curves).

Results of several sets of measurements of pickup amplitude and harmonic content as a function of tracking force are shown in Fig. 11 as solid lines and dot-dash lines. Both audio (97 Å p-p, approx. 1 μm wavelength) and video (800 Å p-p, approx. 7 μm wavelength) signals were measured. The scale for the dot-dash lines is arbitrary since no absolute capacitance calibration was made for this set of

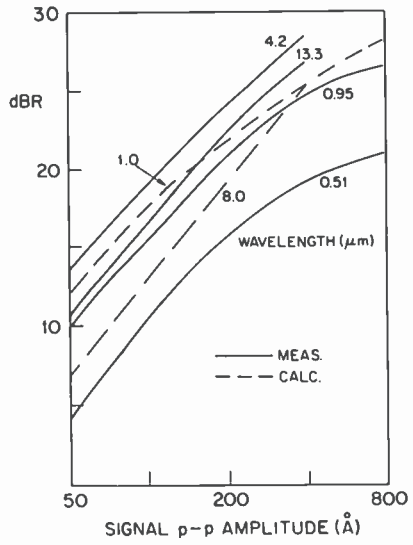

Fig. 9—Amplitude dependence of pickup at different wavelengths in μm (solid curves are measured values, dashed lines are calculated values).

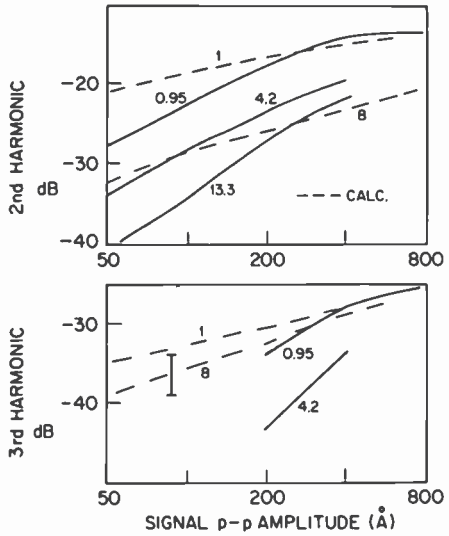

Fig. 10—Harmonic content of pickup as a function of signal amplitude (solid curves are measured values, dashed lines calculated values). Wavelength in μm on curves.

measurements; the video response has been placed close to that of the other data. The tracking-force dependence of the audio response shown by one of the solid lines can be seen to differ significantly from that of the other curves, more in fact than the error bars which show the data point scatter. The open circles shown are single points from another set of measurements at 65 dyne. It is evident that there is a considerable spread in the experimental data, produced by factors whose nature has not been determined.

Corresponding calculations of pickup amplitude and second harmonic dependence on tracking force are shown in Fig. 11 as dashed lines. An effective shoe length of 4 μm has been used, together with an electrode gap of about 500 Å, which gives an audio pickup amplitude within the range measured. The calculated tracking-force dependences, the audio/video ratio, the second/third harmonic ratios, are all consistent with the type of measured behavior. Variations in tracking-force dependence of measured audio pickup are consistent with the variations calculated in Fig. 7 for different shoe set-back values. The comparison therefore gives some plausibility to the model, even if a close correspondence cannot be made.

Fig. 12 shows the tracking-force dependence of the 5 MHz, 2 MHz, and 8 MHz signals. These measurements are shown as dashed lines

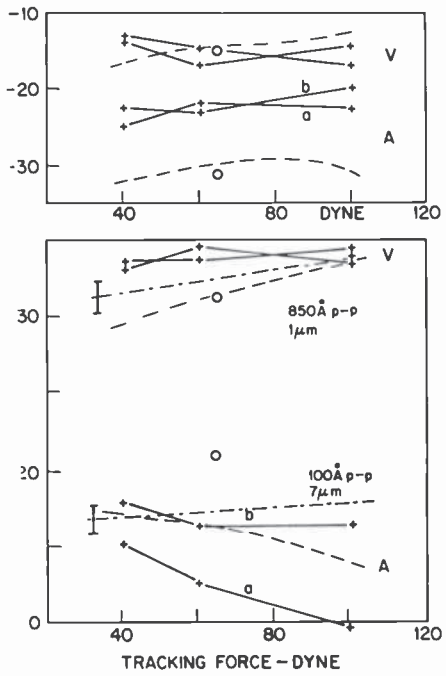

Fig. 11—Pickup amplitude and harmonic content as a function of tracking force for video (850 Å, 1 μm wavelength) and audio (100 Å p-p, 7 μm wavelength) signals. The solid lines, dot-dash lines, and circles are measured values; the dashed lines are calculated values. An arbitrary dB zero is used for the dot-dash curves.

with error bars to indicate scatter of the measured points; the absolute amplitude scale for the whole set again, is arbitrary. The solid curves show the result of present calculations with the same shoe as in Figure 11; the variation of the calculated curve slope with signal frequency is consistent with that measured.

Soundbeat

Details of the mechanism generating soundbeat are quite subtle and the way in which it may vary with various pickup parameters is not intuitively obvious. Understanding of the soundbeat mechanism is gained if two separate components of the change of capacitance, before and after the stylus-electrode plane, are considered separately. It then becomes apparent that the soundbeat of each individual component is less than that of the combination. There is,

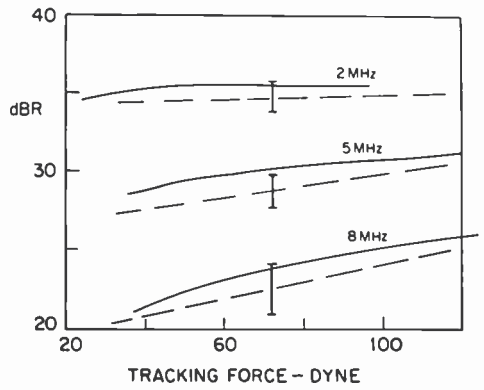

Fig. 12—Dependence of pickup on tracking force at three signal frequencies (5 MHz = 1 μm wavelength). Solid curves are for calculated values and dashed lines for measured values (arbitrary dB zero). Measurement error is indicated.

however, an amplitude modulation at the audio frequency that is different for the two parts, being less for the forward part which is compressed under the shoe. Since there is a substantial phase-shift between the two parts, the amplitude modulation translates to a phase modulation in the total pickup. This is to be contrasted with the situation of a stylus on a rigid, undeformed signal contour. Here the amplitude modulation of the two parts is of similar magnitude; when they are summed, the net phase modulation is small. Fig. 13 shows the after and before parts (A and F) and the total (T) calculated capacitance modulation for a deformed contour; the larger amplitude modulation of the after part can be seen. The upper trace (S) is the bandpass filtered signal, where the audio component and the harmonics have been removed from the T trace. The soundbeat is too small to be visible on this scale.

Table 3 gives the modulation for a typical signal-stylus combination with 85 Å p-p audio, for normal disc elasticity and tracking force and also for a rigid contour (equivalently obtained by setting a zero tracking force). The electrode gap has been adjusted to give approximately similar pickup amplitude in each case. With the normal situation, the video amplitude modulation depths are 0.2 dB and 0.9 dB before and after the electrode, respectively. This small difference, together with the video phase shift of 0.187 of a cycle, is the primary cause of the soundbeat, which is 4.6 dB greater than the average of the two parts. In comparison with this, for the rigid contour, the amplitude modulation of both parts of the video signal is the same (1.5 dB), so there will be no extra component

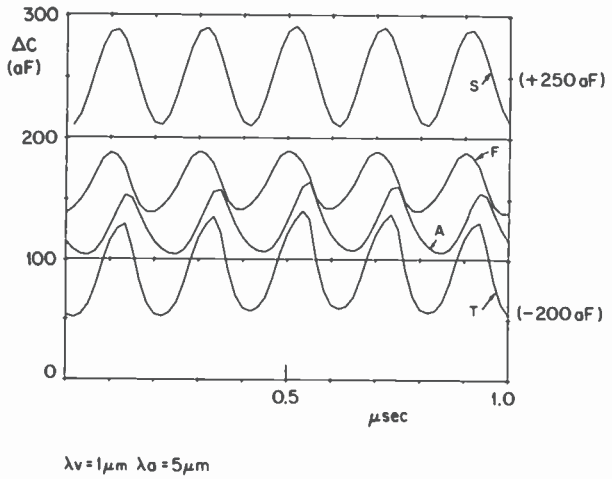

Fig. 13—Calculated components of total pickup from before (F) and after (A) the stylus/electrode plane. The total signal (T = A + F) is shown bandpass filtered in the upper trace (S).

added to the soundbeat of the individual parts. The phases of the individual parts, however, are opposed, being 0.40 and −0.11 of a cycle respectively. As a consequence, the total computed soundbeat is reduced to −48.6 dB. This difference value will be sensitive to electrode configuration.

When the contour is rigid, the phase modulation of the after part

Table 3—Contribution of Forward and After Parts to the Total Soundbeat (SB) and Pickup Amplitude for Deformed and for Rigid Contours

Part of Stylus Plane	Contour	
	Deformed	Rigid
After		
SB (−dB)	31.9	35.5
(Phase)	0.46	−0.11
Video (dBR)	25.8	27.5
(dB Modulation)	0.9	1.5
(Phase)	0.660	0.649
Forward		
SB (−dB)	31.3	31.7
(Phase)	0.46	0.40
Video (dBR)	25.3	25.3
(dB Modulation)	0.2	1.5
(Phase)	0.473	0.446
Total		
SB (−dB)	27.0	48.6
Video (dBR)	30.0	30.6

is opposite to that of the forward part, because a motion of the disc surface toward the stylus causes greater relative contribution from the capacitance elements near the center plane. The phases of video pickup from the two parts therefore move toward each other. It may then be questioned why this does not happen when the contour is normally deformed. Table 3 shows that the video phase of the after part moves back rather than forward as the surface approaches the electrode at the peak of the audio. The reason is not clear. It must be supposed that the contour distorts in such a way that a compensating phase shift away from the electrode is produced.

Calculations of soundbeat are shown in Fig. 14 for a shoe of effective length 3.5 μm and a profile matched to SEM measurement of a normal shoe. These are compared with scattered values measured using a number of standard styli with similar shoe lengths, averaging about 4.5 μm overall, and a test disc with an audio amplitude of 85 Å p-p and a video wavelength of approximately 1 μm. The three calculated points in Fig. 14 correspond to three different electrode gaps. The points are seen to lie well within the scatter of measurements but about 1 dB lower than the mean. The drop of soundbeat with increased pickup is consistent with measurement, although the scatter is too great to give this any real significance.

Two sets of measurements of the dependence of soundbeat on signal wavelength are shown in Fig. 15(a). Both sets used test discs in which the signal frequency remains constant, so that the wavelength varies as the playing radius changes. In all cases the audio amplitude was 100 Å p-p and the video 850 Å p-p; the video fre-

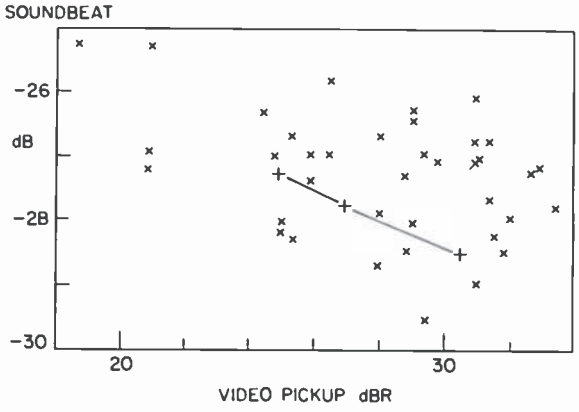

Fig. 14—Calculated soudbeat (solid line) as a function of pickup change caused by electrode-gap variation compared with measurements using a number of standard styli.

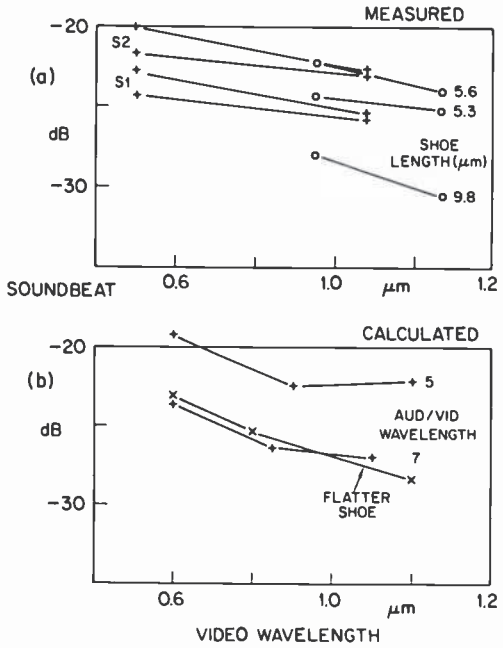

Fig. 15—Soundbeat for normal signal as a function of wavelength: (a) measured values of soundbeat for different shoe lengths (values shown by crosses are from R. W. Nosker; circles are from this study (uncertain dB zero)); (b) calculated values for video output level similar to measured values for different audio/video wavelength ratios.

quency was 5 MHz and the audio less by a factor of 7 (S1 signal) or of 5.6 (S2 signal). The steeper lines of the measurements shown by crosses were made with a flatter stylus shoe. Lines shown by circles (S1 signal only) include a small estimated correction for the zero offset of the whole group.

Calculated curves corresponding to these measurements are shown in Figure 15(b). Again, the stylus shoe profile was taken as approximating those seen in SEM and the electrode spacing adjusted to give the magnitude of video pickup that was measured. The shorter-wavelength audio signal in the calculations had only 5 times the video wavelength and so does not correspond exactly to the S2 factor of 5.6. Measurement and calculation are in reasonable agreement, although there is still a tendency for calculated soundbeat values for the normal length shoe to be about 1 dB lower than measured; changes of stylus profile, shoe length, or electrode

spacing within a reasonable range did not increase soundbeat significantly above values in Fig. 15(b).

The points marked "flatter shoe" were calculated for a shoe with curvature 0.7 of that used in the other curves; it shows a stronger wavelength dependence, as in the measurements. Calculations for an 8 μm shoe show little change of soundbeat from the normal-length shoe if the shoe is level, which is in contrast to the 7 dB drop measured for the 9.8 μm real shoe compared to a 5 μm real shoe (plots c versus a and b in Fig. 10(a)). The reason for this may be the higher sensitivity of the longer shoe to shoe tilt, that is, to a slightly prow-down condition. A further calculation using a shoe that is 200 Å prow-down, corresponding to the tilt produced by a rise in record level of only 4 mils, shows a dramatic drop in soundbeat, on the order of 10 dB. This is primarily due to the drop of stylus pressure near the electrode as the shoe tilts to a prow-down condition. For a normal length shoe, the effect is calculated to occur only for much larger tilts.

Finally, the effect of a flat-top signal may be noted. Soundbeat can be reduced by modifying the waveform so that all signal contour peaks are at the same level:

$$A = A_o \cos k_a x + (A_v - A_a \cos k_a x) \cos k_v x$$

Table 4 shows the soundbeat calculated for this waveform, for an S1 audio signal of 85 Å p-p amplitude ($2A_o$), and a shoe of curvature factor 1.5 compared with that for a normal signal. The reduction of soundbeat is substantial: 7.5 dB for electrode E2 (Table 2), which gives a normal video signal output level, and 9.3 dB for E1, which is close-spaced and gives a signal about 4 dB above normal. Measurements with the same three styli as Fig. 15(a) for a flat-top signal with a nominal 100 Å p-p audio component gave soundbeat values that were lower and had a dependence on video wavelength in the opposite direction to that of a normal signal. Calculated

Table 4—Effect of Flat-top Signal on Soundbeat (SB) for Electrodes E1 and E2 (See Table 2)

	E1		E2	
Signal	SB (−dB)	Video (dBR)	SB (−dB)	Video (dBR)
Normal	27.7	33.5	28.0	29.4
Flat	37.0	33.5	35.5	29.4

values have a similar dependence on wavelength but a magnitude that represents an approximately 3 dB greater reduction from the normal signal. This difference may be due to the way in which the disc signal is produced. Even though a flat-top electrical signal was fed to the cutter head that made the original master, the cutting process may be sufficiently nonlinear to reintroduce some added audio signal.

Conclusions

The general agreement of the calculations with measurement confirms the broad validity of the contour deformation model of stylus pickup. Many of the apparent discrepancies can be seen to lie within the scatter of experiment or to involve unknown factors, such as the linearity of the signal-cutting mechanism. Agreement is best when an electrical calibration is not involved, as in the dependence on tracking force. A more extensive and correlated set of measurements would be required to elucidate the effect of all stylus and disc parameters and obtain a complete understanding of the limitations of the model.

Acknowledgements

The author is indebted to C. H. Anderson, R. W. Nosker and J. R. Matey for a number of informative discussions on the basic physical concepts of this analysis; to R. W. Klopfenstein for showing the method of solution for the pressure distribution; and to J. J. Gibson for discussion of alternate analyses and for the design of the flat-top signal geometry. The various measurements quoted have been made, at varying locations within RCA, by D. Brigham, J. E. Economou, J. R. Matey, R. W. Nosker, J. G. Pecorari, and E. D. Simshauser, with the assistance of G. R. Auth and J. F. McLaughlin; their contribution to this paper is gratefully acknowledged.

References:

[1] J. K. Clemens, "Capacitive Pickup and the Buried Subcarrier Encoding System for the RCA VideoDisc," *RCA Rev.*, 39, p. 33, March 1978.
[2] S. P. Timoshenko and J. N. Goodier, *Theory of Elasticity*, 3rd Edition, McGraw-Hill Book Co., p. 402.